Reaching law-based SMC for spacecraft applications with actuators constraints

Reaching law based SMC for spacecraft applications with actuators constraints

Mauro Mancini[1] and Elisa Capello[2]

***Abstract*— This paper considers a robust sliding mode control method for a spacecraft attitude control. The design of the control law is based on the reaching law approach for continuous-time systems. A novel method is proposed to design the parameters of both the reaching law and the sliding surface. The reaching law ensures that during the reaching phase the states of the system remains bounded. Then, taking into account the parameters of the mathematical model, the bounds are defined so that the control law does not overload the actuator limits, whatever the initial conditions. Furthermore, a variable gain is considered for the control law, to provide chattering alleviation of the control input. Numerical simulations are performed to show the effectiveness of the proposed approach.**

I. Introduction

Attitude Control System (ACS) has a fundamental importance in space missions. In order to ensure that the spacecraft achieves the mission objectives, ACS must guarantee precise pointing accuracy, fast maneuvering, low control effort and robustness against parametric uncertainties and external disturbances [1]. Reaction wheels are widely used as actuators for ACS, since a minimum set of three wheels can provide a 3-axis active control with high pointing accuracy without using a consumable propellant [2]. Despite the great benefits that reaction wheels present, there are some issues on the performance that these actuators can develop. Firstly, there are structural constraints on the maximum rotational speed of the wheel, i.e. there is a maximum angular momentum that can be stored into the wheel [3]. Given the purposes of ACS, reaction wheels can be actuated either to perform an attitude maneuver or to counteract a non-conservative torque acting in the system. In both cases there is an accumulation of angular momentum stored into the wheel, which can lead to saturation of the actuator, i.e. it can no longer store any angular momentum [4]. This situation may arise if the maneuver is performed at a high angular speed or if a secular external torque acts on the spacecraft [5], [6]. In both cases, if a reaction wheel is saturated, it can not accelerate further, which means that the spacecraft can not be controlled around the axis of the saturated wheel. Due to the secular non-conservative torques, this condition can occur during the space mission. For this reason, a spacecraft is equipped with devices to provide momentum dumping, i.e. thrusters or magnetorquers [7]. On the other hand, a well designed ACS should ensure that the actuators do not saturate during the maneuver, to successfully complete it. The second issue for ACS concerns the torque exchanged between the wheels and the spacecraft. In fact, the torque developed by the brushless electric motor is closely related to the electrical power required to drive it [8]. Moreover, on one hand there is a saturation value on the maximum torque supplied, and on other hand the ACS must ensure low control effort, so that the on board electrical power suffices to achieve real-time 3-axis control [9]. Constraints on the saturation of the actuators and the need for low energy consumption complicate the design of the ACS, which already has the inherent difficulty of dealing with a non-linear system such as the spacecraft's attitude dynamics. The nonlinearity of the model can be handled by a nonlinear control system. In this paper, the main objective is to design a Sliding Mode Control (SMC) algorithm, in which the actuator constraints are included.

SMC are nonlinear control techniques with remarkable properties of precision, robustness, tuning, and ease of implementation. In SMC a generic n^{th}-order non-linear system with l inputs is replaced by an equivalent $n-l$ order problem, as in [10]. The equivalent control problem can be obtained designing the SMC controller in two steps: (I) a sliding variable is defined as a function of the system output and its time derivatives, (II) a discontinuous control law is defined to force the system trajectory. When the sliding variable is equal to zero, the trajectories of the system are enclosed in domain named sliding surface, ensuring that the output of the system can reach the desired target. Then, the system trajectory, as previously said, is forced to reach the sliding surface and to remain on it in spite of the uncertainties and perturbations [11]. Starting from any initial condition, there is a phase, named *reaching phase*, in which the system trajectories reach the sliding surface. Then, they move along the sliding surface during the *sliding phase*, and the error tends to zero exponentially [12]. So, during the *sliding phase*, the trajectories of the system are enclosed in the domain of the sliding surface and they are insensitive to perturbations, but these properties are lost during *reaching phase*. In this first stage of SMC, the states of the system are unconstrained and the trajectories are sensitive to perturbations [13]. Therefore, a control gain must be defined to overcome the perturbations in order to bring the system towards the sliding surface. In [14], a barrier function is defined to avoid control gain overestimation. However, the states of the system are not limited during the reaching phase and, for example, the reaction wheels could saturate in this phase. A widely used method to deal with reaching phase is the *reaching law approach* [15], [16]. This approach consists

[1]M. Mancini is with the Department of Mechanical and Aerospace Engineering, Politecnico di Torino, Corso Duca degli Abruzzi 24, 10129 Torino, Italy,

[2]E. Capello is with the Department of Mechanical and Aerospace Engineering, Politecnico di Torino and with the CNR-IEIIT, Politecnico di Torino, Corso Duca degli Abruzzi 24, 10129 Torino, Italy

of first setting the desired evolution of the sliding variable, i.e. the *reaching law*. Then, the control signal is designed so that the system follows the established reaching law during the reaching phase. In this work, a suitable reaching law is derived for ACS problem. Then, a novel strategy is used to define the parameters of both the reaching law and the sliding surface. Taking into account the saturation values of the actuators, this strategy successfully avoid the saturation problem. In addition, an innovative rule is proposed to adjust on-line the parameters of the reaching law according to the system states. The aim of this gain variation is to alleviate the chattering in the command line due to control law discontinuity. Then, this strategy is validated by extensive simulations performed with a three degree-of-freedom (DOF) orbital simulator.

The paper is organized as follows. The mathematical models for both the attitude dynamics and kinematics of the spacecraft and the problem of reaction wheels saturation are presented in Section II. The SMC based control laws able to provide chattering avoidance and to avoid actuator saturations is derived in Section III. In the same section, a proof of the Lyapunov stability is also presented. The numerical example and the simulation results are introduced in Section IV. Finally, some concluding remarks are described in Section V.

II. MATHEMATICAL MODELS

This section provides the mathematical models used to simulate the attitude dynamics and kinematics of a spacecraft actuated by reaction wheels. For this purpose, two different reference frames are defined: (I) $\mathscr{F}_I = (x_I, y_I, z_I)$ is the inertial reference system [17] and (II) $\mathscr{F}_B = (x_B, y_B, z_B)$ is fixed to the spacecraft. The spacecraft is supposed to be rigid and with three principal central axes of inertia, which are aligned to the body reference frame. Instead, reaction wheels are arranged in a cluster whose center of mass is coincident with the spacecraft's center of mass. Furthermore, each wheel has its rotation axis aligned with a principal central axis of the spacecraft. So, each wheel provides active control around one axis of the body frame and a full 3-axis active control is achieved.

A. System dynamics

The spacecraft attitude dynamics is described by the Euler's equation

$$J\dot{\omega} + \omega \times \left(J\omega + h_{\text{rw}}\right) = \tau + d, \tag{1}$$

where $\dot{\omega}, \omega \in \mathbb{R}^3$ are the vectors of the angular accelerations and angular velocities of the spacecraft with respect to inertial frame. $J \in \mathbb{R}^{3,3}$ is the inertia matrix of the spacecraft and it is diagonal. $d \in \mathbb{R}^3$ is the external non-conservative torque due to disturbances acting on the spacecraft. Finally, $h_{\text{rw}}, \tau \in \mathbb{R}^3$ are related to the actuation system (i.e. reaction wheels). In fact, τ is the torque provided by the reaction wheels, that represents the spacecraft actuation input provided by the controller, while each component of h_{rw} is the angular momentum stored into a single wheel. Then, τ and h_{rw} are linked by the following relationship [18]

$$\dot{h}_{\text{rw}} = -\tau. \tag{2}$$

Since τ is an internal conservative force, if $d = 0$ the angular momentum of the system is constant over time, i.e. $J\omega + h_{\text{rw}} = \text{constant}$. So, if reaction wheels are started with zero angular momentum and ACS has to keep the attitude inertially fixed, the angular momentum h_{rw} is different from zero only during the maneuver, and the stored angular momentum (by the reaction wheels) is $h_{\text{rw,m}} = -J\omega$. Now, the case in which d is different from zero is analyzed. The role of ACS is to counteract the external disturbance, so the the surplus of angular momentum injected into the system by the external non-conservative torque is absorbed by the wheels. This quantity of angular momentum is indicated by $h_{\text{rw,d}} = \int_0^t d(t)dt$.

Lemma 1: It is assumed that both the desired and initial system states are given by an arbitrary angular position and a zero angular speed. So, ACS must keep the spacecraft inertially fixed. Besides, it is assumed that the reaction wheels are started with zero angular speed, so the system has initially zero angular momentum.

From Lemma 1, it follows that the angular momentum permanently stored into the wheels is only due to the external disturbance d, while $h_{\text{rw,m}} \neq 0$ only during the maneuver. So, we have $h_{\text{rw,m}} + J\omega = 0$ and Eq. (1) can be rewritten as follows

$$J\dot{\omega} = \tau + \xi \quad \xi = -\omega \times \left(h_{\text{rw,d}}\right) + d. \tag{3}$$

B. Actuators saturation

As highlighted in the Introduction, τ and h_{rw} suffer from saturations, i.e. in each wheel these quantities cannot exceed an absolute maximum value. Note that the three wheels are equal to each other, so the outcome is

$$\max|\tau_i| = \bar{\tau} \quad \max|h_{\text{rw}_i}| = \bar{h} \quad i = x_B, y_B, z_B$$

where $\bar{\tau}, \bar{h}$ are the saturation values of the torque and the angular momentum, respectively. Then,

$$\tau_i \in [-\bar{\tau}, \bar{\tau}] \quad h_{\text{rw}_i} \in [-\bar{h}, \bar{h}] \quad i = x_B, y_B, z_B$$

Furthermore, as in the previous Subsection, the maximum speed allowed for the spacecraft during the maneuver $\bar{\omega}$ is derived to avoid angular momentum saturation of the wheels. This value is function of both $\bar{h}$ and the angular momentum accumulated in the wheels before the beginning of the maneuver $h_{\text{rw,d}}$ according to

$$\bar{\omega}_i = \frac{\bar{h} - |h_{\text{rw,d}_i}|}{J_{ii}} > 0 \quad i = x_B, y_B, z_B \tag{4}$$

It follows that, to avoid saturations on the angular momentum of the wheels, the angular speed of the spacecraft must respect the following conditions during the maneuver

$$\left|\omega_i\right| \leq \bar{\omega}_i \quad \omega_i \in [-\bar{\omega}_i, \bar{\omega}_i] \quad i = x_B, y_B, z_B \tag{5}$$

Finally, the additional angular momentum accumulated in the wheels during the maneuver to counteract the external

disturbance has been neglected in Eq. (4). However, this is acceptable if the maneuver is sufficiently fast. In fact, this quantity is given by $\int_{t_m} d(t)dt$, where t_m is maneuver time.

C. Attitude kinematics

The orientation of the body frame $\mathscr{F}_B$ with respect to the inertial frame $\mathscr{F}_I$ is expressed by the vector of Euler's angles $\Phi = [\phi, \theta, \psi]^T$. Then, the relationship between the derivative of Euler angles and the body angular velocities ω is

$$\dot{\Phi} = B\omega, \tag{6}$$

as in [4] and with

$$B = \frac{1}{c\theta}\begin{bmatrix} c\psi & -s\psi & 0 \\ c\theta s\psi & c\theta c\psi & 0 \\ -s\theta c\psi & s\theta s\psi & c\theta \end{bmatrix}$$

III. CONTROL STRUCTURE DESIGN

The control algorithms to steer the attitude of the spacecraft described by the equations in Section II are derived in this section. First of all, note that the inertia matrix J of the spacecraft is diagonal, due to the assumption that it has three central axes of inertia. Therefore, in the rotation dynamics each DOF has a dedicated control channel. Thus, in this work a control law is derived separately for each axis of the system $\mathscr{F}_{\mathscr{B}}$. For each axis, we follow the same procedure. So, we first define the sliding surface and the reaching law. From the reaching law, the control law is derived to ensure the system is able to reach the sliding surface while avoiding saturation of the actuators.

A. Sliding surface

First of all, the states errors are defined as

$$\Phi_{e,i} = \Phi_i - \Phi_{d,i} \quad \omega_{e,i} = \omega_i - \omega_{d,i} = \omega_i \quad i = x_B, y_B, z_B$$

where $\Phi_{d,i}, \omega_{d,i}$, $i = x_B, y_B, z_B$ are the desired angular positions and angular velocities respectively, while Φ_i, ω_i are the states of the systems, whose derivatives are given by Eqs. (6) and (1) respectively. $\omega_{e,i}$ is obtained from Lemma 1. Since the ACS problem for each axis of the spacecraft is a second-order dynamic system, the following conventional sliding surface is used

$$s_i = \omega_i + \lambda_i \Phi_{e,i} \quad \lambda_i > 0 \quad i = x_B, y_B, z_B \tag{7}$$

For this second-order system the sliding surface can also be presented as follows [10]

$$s_i = \left(\frac{d}{dt} + \lambda_i\right)\Phi_{e,i} \quad i = x_B, y_B, z_B \tag{8}$$

B. Reaching law

In this work, a novel reaching law is introduced and specified for the attitude dynamics of a spacecraft. The starting point is the *constant rate reaching law* initially presented in [15]

$$\dot{s} = -Q \ \mathrm{sgn}(s) \quad Q > 0. \tag{9}$$

Looking at Eq. (9), a compromise is required for the choice of Q parameter, and this should be a drawback. In fact, high Q values increase the speed of convergence towards the sliding surface, but at the same time they cause an increase in chattering during the sliding phase. In addition, if the Q parameter is not properly tuned, it can lead to excessive magnitude of the control signal and state variables during the reaching phase. So, in this paper, the constant coefficient Q in Eq. (9) is replaced by a variable gain k, the value of which is defined by an appropriate function of s, i.e. $k = k(s)$. The aim is to ensure that, through the variable gain, Eq. (9) can provide a satisfactory convergence speed even with the chattering phenomenon. Then, k is given by

$$k_i = \bar{k}_i \ \frac{\arctan\left(G_i|s_i|\right)}{\pi/2} > 0 \quad \forall \ s_i \quad i = x_B, y_B, z_B \tag{10}$$

It can be seen that $k_i < \bar{k}_i \ \forall \ s_i$, so $\bar{k} > 0$ is an upper bound. As detailed later, this gain is defined to avoid actuator saturations, instead the gain G determines the value of s for which k approaches $\bar{k}$. Then, the new reaching law for the ACS is introduced taking into account Eq. (3)

$$\dot{s}_i = -k_i \ \mathrm{sgn}(s_i) + \xi_i \quad i = x_B, y_B, z_B \tag{11}$$

C. Control law

Now, the structure of the control law is derived to drive the dynamic system towards the sliding surface, i.e. where $s_i = 0$, $i = x_B, y_B, z_B$.

Remark 1: The domain of the space defined by $s_i = 0$ is not subject to any transformation if Eq. (7) is multiplied by a constant $C_i > 0$.

As a result of Remark 1, it is possible to select $C_i = J_{ii}$, $i = x_B, y_B, z_B$, and the sliding surface can be written as

$$s_i = J_{ii}\omega_i + \lambda_i J_{ii}\Phi_{e,i} \quad \lambda_i > 0 \quad i = x_B, y_B, z_B \tag{12}$$

or

$$s_i = \left(\frac{d}{dt} + \lambda_i\right)J_{ii}\Phi_{e,i} \quad i = x_B, y_B, z_B \tag{13}$$

Lemma 2: In order to derive the control law, it is assumed that $\dot{\Phi}_i = \omega_i$, with $i = x_B, y_B, z_B$.

Thanks to Lemma 2 and Eq. (3) the time derivative of Eq. (12) is given by

$$\dot{s}_i = \lambda_i J_{ii}\omega_i + \tau_i + \xi_i \quad i = x_B, y_B, z_B \tag{14}$$

Then, the control law, which ensures the system is governed by the reaching law in Eq. (11) during reaching phase, is obtained from Eqs. (11) and (14)

$$\tau_i = -k_i \ \mathrm{sgn}(s_i) - \lambda_i J_{ii}\omega_i \quad i = x_B, y_B, z_B \tag{15}$$

D. Control parameters design

Now, the strategy to define the parameters of the controller is synthesized. These parameters are the upper bound of the control gain $\bar{k}_i$ in Equation (10) and the slope of the sliding surfaces λ_i, $i = x_B, y_B, z_B$. As mentioned earlier, the most significant outcome of this strategy is to avoid actuator saturation. First of all, it is important to point out that reaching law in Eq. (11) has a bound, because it

is $k_i \text{sgn}(s_i) \in (-\bar{k}_i, \bar{k}_i)$ from Eq. (10). Furthermore, ξ also consists of two bounded terms. Indeed, d is usually due to external non-conservative torques produced by orbital perturbations, and they are bounded [4], [19], while $h_{\text{rw,d}}$ is bounded by saturation constraints. Finally, if the initial system states respect the condition in Eq. (4), then the control law synthesized in this work succeeds to maintain the system within limits imposed by the same condition. It follows that it is possible to define a bound for ξ: $|\xi_i| \leq \mu_i$, $i = x_B, y_B, z_B$. Then, when the system dynamics is ruled by Eq. (15), for any s_i it is obtained that

$$|\dot{s}_i| < \bar{k}_i + \mu_i \quad i = x_B, y_B, z_B \tag{16}$$

Then, differentiating Eq. (13) with respect to time, we have

$$\dot{s}_i = \left(\frac{d}{dt} + \lambda_i\right) J_{ii}\omega_i \quad i = x_B, y_B, z_B \tag{17}$$

As is pointed out in [10], [20], Eq. (17) reveals that $J_{ii}\omega_i$ is obtained as the output of a first-order linear filter fed with $\dot{s}_i$. Thus, taking into account Eq. (16) and the initial conditions of the system, it is possible to conclude that the output of first order filter is bounded as follows

$$|\omega_i| < \frac{\bar{k}_i + \mu_i}{J_{ii}\lambda_i} \quad i = x_B, y_B, z_B \tag{18}$$

Since ω_i must satisfy Eq. (5), to avoid the saturation of the reaction wheels angular momentum, it follows that

$$\frac{\bar{k}_i + \mu_i}{J_{ii}\lambda_i} \leq \bar{\omega}_i \quad \Rightarrow \quad \lambda_i \geq \frac{\bar{k}_i + \mu_i}{J_{ii}\bar{\omega}_i} \quad i = x_B, y_B, z_B \tag{19}$$

From Eq. (19) we define values of λ_i that ensures the compliance of constraint in Eq. (5), guaranteeing no saturation of the angular momentum of the wheel. To compute λ_i, the bound $\bar{k}_i$ should be established. As briefly mentioned above, this bound is defined without saturation of the wheel torque, so $\tau_i \leq \bar{\tau}\ \forall\ s_i$. Then, from Eq. (15), we have

$$\left|\tau_i\right| < \bar{k}_i + \left|\lambda_i J_{ii}\omega_i\right| < \bar{k}_i + \left|\lambda_i J_{ii}\bar{\omega}_i\right| \quad i = x_B, y_B, z_B \tag{20}$$

Now, as in Eq. (19), λ_i is substituted in the last of Eq. (20),

$$\left|\tau_i\right| < \bar{k}_i + \frac{\bar{k}_i + \mu_i}{J_{ii}\bar{\omega}_i} J_{ii}\bar{\omega}_i = 2\bar{k}_i + \mu_i \quad i = x_B, y_B, z_B \tag{21}$$

Finally, the choice of the upper bound $\bar{k}_i$ is given by, ensuring that wheel torque saturation is avoided

$$\bar{k}_i \leq \frac{\bar{\tau} - \mu_i}{2} \quad i = x_B, y_B, z_B \tag{22}$$

E. Proof of stability

In order to provide the asymptotic stability of the dynamics system about the equilibrium point $s_i = 0$, the control law must guarantee the following condition [12]

$$s_i \dot{s}_i < 0 \quad i = x_B, y_B, z_B \tag{23}$$

Thus, Eqs. (3), (10), (12), (15) are introduced in Eq. (23) to obtain

$$\begin{aligned} s_i\left(\lambda_i J_{ii}\omega_i + \tau_i + \xi_i\right) &= s_i\left(-\bar{k}_i\ \frac{\arctan\left(G_i|s_i|\right)}{\pi/2}\text{sgn}(s_i) + \xi_i\right) \leq \\ &\leq |s_i|\left(-\bar{k}_i\ \frac{\arctan\left(G_i|s_i|\right)}{\pi/2} + \mu_i\right) \quad i = x_B, y_B, z_b \end{aligned} \tag{24}$$

So, to verify that the control law (15) is able to steer the dynamics system (1) to the sliding surface domain, with k defined by Eq. (10), the last term of Eq. (24) has to be negative for all $s_i \neq 0$. First of all, the upper bound of the control gain must be greater then the bound of the perturbation terms: $\bar{k}_i > \mu_i$, $i = x_B, y_B, z_B$. Together with Eq. (22), this leads to a constraint on the choice of the actuators. In fact, they must provide a maximum torque given by

$$\frac{\bar{\tau} - \mu_i}{2} > \mu_i \Rightarrow \bar{\tau} > 3\mu_i \tag{25}$$

Then, Eq. (10) is introduced to avoid chattering of the command lines near the sliding surface. Still, the role of Eq. (10) is to introduce a boundary layer around the sliding surface where the switching control is smoothed out, thus a boundary layer sliding mode is obtained [10]. In fact, since $k_i \to 0$ if $s_i \to 0$, this novel reaching law can not longer guarantee convergence of the system state to the sliding surface, but only to a band around $s_i = 0$. Then, as mentioned above, the thickness of the boundary layer can be adjusted by the parameter G_i. In fact, this parameter can modify the shape of the arctangent function, and so it allows to set the value $\pm\bar{s}_i$, $\bar{s}_i > 0$ at which $k_i \simeq \bar{k}_i$, and so the condition (23) is achieved. Then, for $|s_i| < \bar{s}_i$ the value of k_i decreases faster the larger G_i is, therefore the condition (23) can not longer be guaranteed for $|s_i| < \bar{s}_i$. So, the boundary layer is defined as

$$B_i = \left\{[\Phi_{e,i}, \omega_i] : |s_i| < \bar{s}_i\right\} \quad i = x_B, y_B, z_B$$

IV. NUMERICAL EXAMPLE

In this section, numerical simulations are conducted through *Matlab* software to demonstrate the performance of the proposed control strategy. The dynamic system is given by Eqs. (1), (2), (6) and a targeting maneuver is considered as a reference. Therefore, at the initial step, the spacecraft is affected by an attitude error, which must be steered to zero by the control system. Then, when the zero error is reached, the attitude must be kept constant. Thus, performance are evaluated (I) on the accuracy with which the control law achieves the desired attitude and (II) on the ability of the control law to ensure that the reaction wheels do not saturate during the maneuver. The parameters of the dynamic systems and the initial and objective conditions are listed in Table 1. The initial angular momentum stored in the reaction wheels is due to the action of the secular disturbance torques d acting on the system, as explained in Section II. Then, the bounds on the angular velocity at which the maneuver can be carried out are obtained from Eq. (4):

$$[\bar{\omega}_x,\ \bar{\omega}_y, \bar{\omega}_z] = [0.25,\ 1.12,\ 0.75] \cdot 10^{-2} \text{ rad/s}.$$

Table 1 System parameters and initial conditions

$J_{xx} = 6$ kgm^2	$\Phi_0 = [40,\ -30,\ 20]^T$ deg
$J_{yy} = 2$ kgm^2	$\omega_0 = [0,\ 0,\ 0]^T\ \frac{\text{rad}}{\text{s}}$
$J_{zz} = 4$ kgm^2	$\Phi_d = [0,\ 0,\ 0]^T$ deg
$\bar{\tau} = 2 \cdot 10^{-3}$ Nm	$h_{rw,d} = [1.5,\ 0.75,\ 0]^T \cdot 10^{-2}\,\frac{\text{kgm}^2}{\text{s}}$
$\bar{h} = 3 \cdot 10^{-2}\ \frac{\text{kgm}^2}{\text{s}}$	$d = [0.9,\ 0.45,\ 0]^T \cdot 10^{-5}$Nm

Table 2 Control parameters
$[\mu_x, \mu_y, \mu_z] = [2,\ 2,\ 2] \cdot 10^{-4}$ Nm
$[\lambda_x, \lambda_y, \lambda_z] = [7.33,\ 4.89,\ 3.67] \cdot 10^{-2}$
$[\bar{k}_x, \bar{k}_y, \bar{k}_z] = [0.9,\ 0.9,\ 0.9] \cdot 10^{-3}$
$[G_x, G_y, G_z] = [10^4,\ 10^4,\ 10^4]$

After, the control parameters listed in Table 2 are obtained. The Euler angles are shown in Figure 1. The error in x_B is the slowest to converge to zero, in accordance with the more restrictive bound on the allowed angular velocity and the greater inertia of the spacecraft on this axis. Nevertheless, the control law manages to cancel the initial error on the Euler angles despite the external disturbance torque, with the following final accuracy

$$[\phi,\ \theta,\ \psi]_f = [0.94,\ -0.48,\ -0.04] \cdot 10^{-3} \text{ deg}.$$

Then, Figure 2a shows that the control law succeeds in respecting the constraints imposed on the angular velocities throughout the duration of the maneuver. As explained in detail above, the angular velocities remaining within the bounds ensure that the angular momentum of the wheels does not saturate, as demonstrated in Figure 2b. Instead, the torques provided by the actuators are shown in Figure 3a and it can be seen how the control law manages both to avoid torque saturation and to eliminate chattering in the command line. This last objective is achieved through the variable control gains, which are shown in Figure 4a. Instead, Figure 3b shows the comparison between the control torque and the external disturbance torque for $t \in [350,\ 400]$ s. In this time interval, as it is shown in Figure 1, the spacecraft is at the desired equilibrium point $\Phi_e = 0$, $\omega = 0$. Therefore, the objective of the ACS is to counteract the disturbance torque. Then, Figure 3b shows that the control law is able to compensate the disturbance torque, and thus to keep the spacecraft at the desired equilibrium point. Finally, a comparison between the control gains and the sliding variables for $t \in [350,\ 400]$ s is provided in Figure 4b. As it was pointed out in Section III, the control law (15) is not able to drive the sliding variable s to zero if an external disturbance affects the dynamic system. Indeed, Figure 4b shows that $s_z = 0$ because $d_z = 0$, but $s_x \neq 0$ and $s_y \neq 0$, and this is due to the external disturbances $d_x \neq 0$, $d_y \neq 0$. In fact, by defining $k = k(s)$ as described in Eq. (10), it is possible to smooth out the discontinuity in the control law and thus to avoid chattering in the command line. Nevertheless, the drawback is that $s \to 0$ only for $d = 0$, otherwise, for $d \neq 0$ the result is $|s| \in (0, \bar{s}]$. Then, according to Eq. (10) it can be concluded that $k \to 0$ only if $d = 0$, otherwise, for $d \neq 0$ the result is $k \in (0, k(\bar{s})]$. It can be observed that Figure 4b confirm those results. Now, a comparison with a control structure derived as in [21] is performed, and the same variation law (10) is used for the control gains. In this case, the control law and the sliding surface are respectively

$$\tau_i = \rho\ \text{sign}(\sigma_i) - c\omega_i \quad \sigma_i = \omega_i + c\Phi_{e,i} \quad i = x_B, y_B, z_B \quad (26)$$

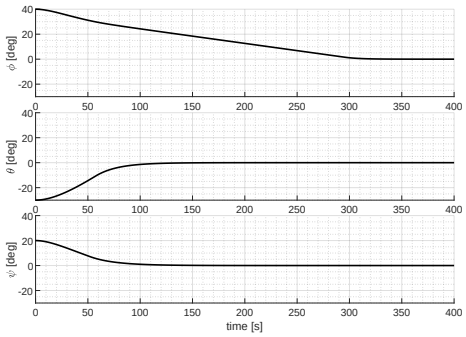

Fig. 1. Euler angles.

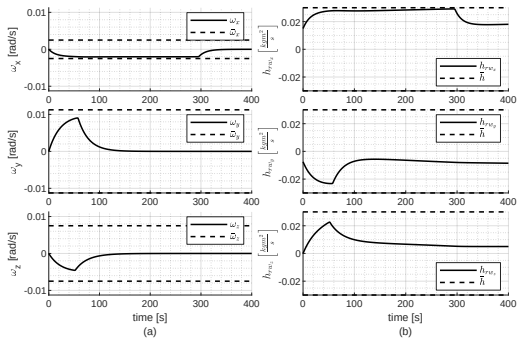

Fig. 2. (a) Angular velocities and (b) Angular momentum of reaction wheels.

Then, the control parameters are defined as $\bar{\rho} = 2 \cdot 10^{-3}$, $c = 0.1$ and the same gain G as in Table 2. The same initial conditions and system parameters of Table 1 are used for the numerical simulations, and Figure 5 shows that in this case the control structure (26) fails to prevent the actuators from saturating during the maneuver. So they are unable to physically realise the output of the control law and the system cannot realise the maneuver in one step. In fact, once the wheels accumulate the maximum amount of angular momentum, it must be dumped so that the wheels can again provide torque and thus the maneuver can continue.

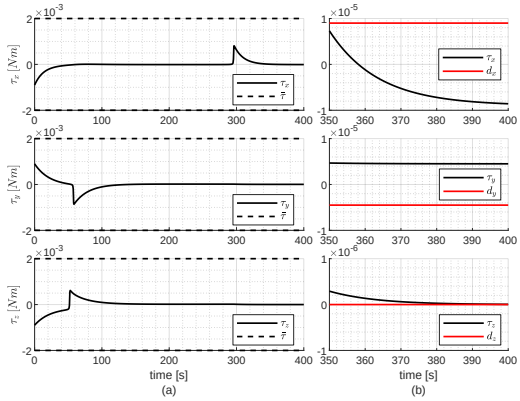

Fig. 3. (a) Control torque. (b) Control torque (black line) vs external disturbance (red line) during the last 50 seconds.

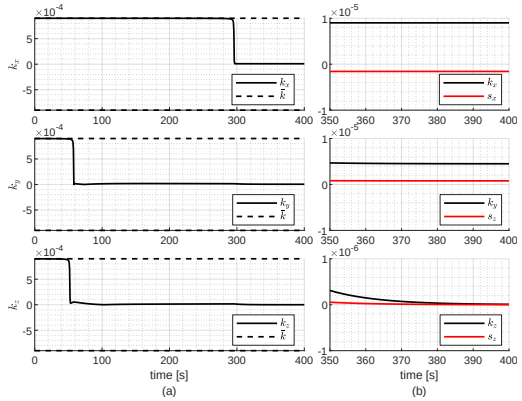

Fig. 4. (a) Control gain. (b) Control gain (black line) vs sliding variable (red line) during the last 50 seconds.

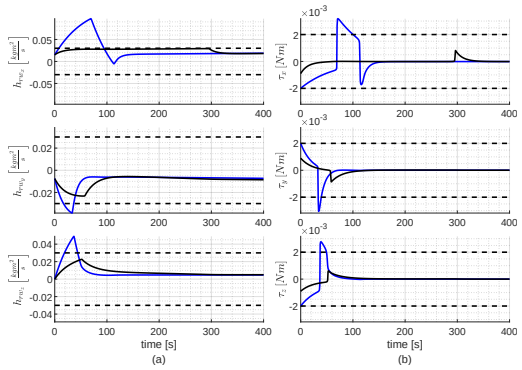

Fig. 5. (a) Angular momentum of reaction wheels and (b) torque variation. Blue line is for classical control law, the black and dotted lines are as in Figure 2b and Figure 3a, respectively.

V. CONCLUSIONS

In this paper, a SMC is designed to manipulate the attitude dynamics of a spacecraft, and the control law is derived starting from the definition of a suitable reaching law. The proposed reaching law introduces a time-varying parameter in the classical *constant rate reaching law* to guarantee a good convergence time towards the sliding surface while avoiding the chattering phenomena. Furthermore, a novel strategy is introduced to define the parameters of the control structure. The key feature of the proposed approach to derive the control law is that it succeeds to avoid saturation of the reaction wheels during the maneuver. The simulation results show that, compared to control structure defined as in [21], the control laws proposed in this paper prevents the reaction wheels from saturation during maneuvering. Thus, the output of the control law defined in this paper can be realised by actuators of a real system, in contrast to the control law in [21]. Moreover, although the control law realises a boundary layer sliding mode, it is able to reach and then maintain the desired attitude with high precision, even under the action of an external disturbance.

REFERENCES

[1] M. J. Sidi, *Spacecraft dynamics and control: a practical engineering approach*. Cambridge university press, 1997, vol. 7.

[2] J. R. Wertz, *Spacecraft attitude determination and control*. Springer Science & Business Media, 2012, vol. 73.

[3] F. A. Leve, B. J. Hamilton, and M. A. Peck, *Spacecraft momentum control systems*. Switzerland: Springer, 2015, vol. 1010.

[4] F. L. Markley and J. L. Crassidis, *Fundamentals of spacecraft attitude determination and control*. New York, NY, USA: Springer, 2014, vol. 33.

[5] A.-R. Luzi, D. Peaucelle, J.-M. Biannic, C. Pittet, and J. Mignot, "Structured adaptive attitude control of a satellite," *International Journal of Adaptive Control and Signal Processing*, vol. 28, no. 7-8, pp. 664–685, 2014.

[6] M. Lovera, "Optimal magnetic momentum control for inertially pointing spacecraft," *European Journal of Control*, vol. 7, no. 1, pp. 30–39, 2001.

[7] X. Chen, W. H. Steyn, S. Hodgart, and Y. Hashida, "Optimal combined reaction-wheel momentum management for earth-pointing satellites," *Journal of Guidance, Control, and Dynamics*, vol. 22, no. 4, pp. 543–550, 1999. [Online]. Available: https://doi.org/10.2514/2.4431

[8] Z. Ismail and R. Varatharajoo, "A study of reaction wheel configurations for a 3-axis satellite attitude control," *Advances in Space Research*, vol. 45, no. 6, pp. 750–759, 2010.

[9] M. Grassi and M. Pastena, "Minimum power optimum control of microsatellite attitude dynamics," *Journal of Guidance, Control, and Dynamics*, vol. 23, no. 5, pp. 798–804, 2000.

[10] J.-J. E. Slotine, W. Li *et al.*, *Applied nonlinear control*. Prentice hall Englewood Cliffs, NJ, 1991, vol. 199, no. 1.

[11] V. Utkin, "Variable structure systems with sliding modes," *IEEE Transactions on Automatic control*, vol. 22, no. 2, pp. 212–222, 1977.

[12] Y. Shtessel, C. Edwards, L. Fridman, and A. Levant, *Sliding mode control and observation*. Springer Science+Business Media, New York, 2014.

[13] E. Tahoumi, "New robust control schemes linking linear and sliding mode approaches," Theses, École centrale de Nantes, Dec. 2019. [Online]. Available: https://tel.archives-ouvertes.fr/tel-02953992

[14] H. Obeid, L. M. Fridman, S. Laghrouche, and M. Harmouche, "Barrier function-based adaptive sliding mode control," *Automatica*, vol. 93, pp. 540–544, 2018. [Online]. Available: https://www.sciencedirect.com/science/article/pii/S0005109818301742

[15] W. Gao and J. C. Hung, "Variable structure control of nonlinear systems: A new approach," *IEEE transactions on Industrial Electronics*, vol. 40, no. 1, pp. 45–55, 1993.

[16] P. Latosiński, "Sliding mode control based on the reaching law approach—a brief survey," in *2017 22nd International Conference on Methods and Models in Automation and Robotics (MMAR)*. IEEE, 2017, pp. 519–524.

[17] E. Canuto, C. Novara, L. Massotti, D. Carlucci, and C. P. Montenegro, "Chapter 2 - attitude representation," in *Spacecraft Dynamics and Control*, ser. Aerospace Engineering, E. Canuto, C. Novara, L. Massotti, D. Carlucci, and C. P. Montenegro, Eds. Saint Louis: Butterworth-Heinemann, 2018, pp. 17–83.

[18] J.-F. Trégouët, D. Arzelier, D. Peaucelle, C. Pittet, and L. Zaccarian, "Reaction wheels desaturation using magnetorquers and static input allocation," *IEEE Transactions on Control Systems Technology*, vol. 23, no. 2, pp. 525–539, 2015.

[19] M. Mancini, N. Bloise, E. Capello, and E. Punta, "Sliding mode control techniques and artificial potential field for dynamic collision avoidance in rendezvous maneuvers," *IEEE Control Systems Letters*, vol. 4, no. 2, pp. 313–318, 2019.

[20] A. Bartoszewicz, "A new reaching law for sliding mode control of continuous time systems with constraints," *Transactions of the Institute of Measurement and Control*, vol. 37, no. 4, pp. 515–521, 2015. [Online]. Available: https://doi.org/10.1177/0142331214543298

[21] M. Mancini, E. Capello, and E. Punta, "Sliding mode control with chattering attenuation and hardware constraints in spacecraft applications," *IFAC-PapersOnLine*, vol. 53, no. 2, pp. 5147–5152, 2020, 21st IFAC World Congress.